Study of resonances in exotic neutron-rich ^{14}Be by the use of isospectral potential

M Hasan [a], M Alam [b], S H Mondal [c], Md A Khan *[d]

[a,b,c,d]*Department of Physics, Aliah University, Newtown, Kolkata-700160, India.*

*drakhan.rsm.phys@gmail.com; drakhan.phys@aliah.ac.in

Abstract. In this work, Hyperspherical Harmonic Expansion (HHE) formalism aided by supersymmetric quantum mechanics is used to study bound and resonant states of ^{14}Be in the three-body (^{12}Be+ n + n) cluster model, and the analysis of the resonant states close to the binding threshold utilizes supersymmetric quantum mechanics (SSQM). GPT nucleon-nucleon potential together with SBB core-nucleon potential is chosen for the solution of three-body Schrödinger equation to get the lowest bound state energy and wave function. In the next stage, energy and wave function of the bound state is used to derive an isospectral potential that exhibit deep well following a strong barrier facilitating confinement (or trapping) of particle inside it at some positive energy (E>0). The trapping probability when plotted against energy shows a prominent peak at the energy of resonance. WKB approximation is used to determine the width of resonance width. Calculated resonance energy and width of resonance are compared with those measured experimentally for the promising neutron halo candidate, the ^{14}Be.

1. Introduction

Significant advancement in the Radioactive Ion Beam (RIB) technologies revealed several exciting features of the nuclei in the neighborhood of nuclear drip-lines. RIB encouraged researchers to study structure of the short-lived, loosely bound exotic nuclei formed near the drip-lines. Discovery of neutron halo structure has opened up new avenues for investigation and substantial theoretical and experimental research has been conducted on the unique structural properties of nuclei linked to the halo phenomenon. The halo can be conceptualized as a threshold phenomenon that occurs when weakly bound valence neutrons penetrate the region far beyond the nuclear core with a high probability. Nuclear halo is characterized by dense core surrounded by weakly bound valence nucleon, far extended one or two-neutron orbitals with low angular momentum, very low nucleon separation energy, large matter radii, and an unusually large interaction cross-section. Investigation of structures of nuclei with large asymmetry in N to Z ratios could provide fresh insights into the NN interactions and few-body dynamics. The two-neutron halo systems have sparked a lot of curiosity and the Borromean halo is another name for it. The two-body components (C-n & n-n) cannot be bound by the close proximity interaction that binds the extensive three-body systems (C-n -n). Resonances and

excited states slightly above the binding threshold are both exciting and scientifically valuable properties of halo nuclei [1-3].

Tanihata and his coworkers are recognized as the first group to confirm the 2n-halo structure in neutron-rich ^{11}Li in 1985, and their work has piqued the interest of the nuclear physics community around the globe [4]. Some of the more intriguing instances of halo nuclei are: confirmed one-neutron halo structure in ^{11}Be [1-5], ^{14}B [6,7], ^{19}C [8-11], ^{31}Ne [12-15], and ^{37}Mg [16,17]; two-neutron halo structure in ^{6}He [18-21], ^{11}Li [22-24], ^{14}Be [25-26], ^{22}C [27-29] , and ^{40,42,44}Mg [30-31]; one-proton halo structure in ^{8}B [32], ^{26}P [33], ^{17}F [34], and two proton halo structure in ^{27}S [35], ^{17}Ne [36].

Special emphasis is now given to ^{14}Be, which is an excellent candidate for having an exotic two-neutron halo structure. The first proof in favor of this comes from studies of interaction cross-sections, reaction cross-sections, and momentum fragment distributions. R. Gilman et al., 1984 [37] found two neutron separation energies (S_{2n}) of ^{14}Be as 1.12 ± 0.16 MeV in pion double charge-exchange studies. J. M. Wouters et al., 1988 [38] determined the S_{2n} of ^{14}Be to be 1.48 ± 0.14 MeV using a time of flight experiment. G. Audi et al., 1993 [39] reported S_{2n} of ^{14}Be as 1.34 ± 0.11 MeV. At RIKEN, Moriguchi et al., 2014 [40] investigated the reaction cross-sections of ^{14}Be with a proton target and concluded that ^{14}Be has a Borromean halo structure. T. Sugimoto et al., 2007 [41] explored the the first excitation of of the ^{14}Be at E_x= 1.54 ±0.13 MeV and ascribed a spin parity $J^{\pi}= 2^+$ from the angular distribution measurement. Korsheninnikov et al., 1997 [42] reported this state at excitation energy, E_x= 1.6 (1) MeV. Using the ^{14}C (^{14}C, ^{14}O) ^{14}Be reaction, Bohlen et al., 1995 [43] identified a candidate for the 2_1^+ state at E_x=1.59 ±0.13 MeV. Kisamori et al., 2016 [44] discovered ^{14}Be resonance behavior and calculated that the mean of the peak at 0.830 ± 0.650 (Sta.) ±1.250 (Sys.).

Here we present an interesting theoretical approach for calculating weakly bound nuclei's resonance states. It requires the existence of a bound ground state as a prerequisite and is capable of handling both bound and resonant states. The approach is founded on the notion that one may derive an isospectral potential family (say, $\hat{w}$) based on a λ free parameter concerning any potential (say, w). When the initial potential consists of a skin-deep well preceded by a low and overly broad barrier (which does not adequately support the resonant states), the parameter may be used to enhance the well's depth and the barrier's height simultaneously. Because $\hat{w}$ and w are precisely isospectral, using these high barriers and deep wells makes it easier to calculate the resonant state properly has an energy equal to that of the initial shallow potential.

We employ the above scheme to explore the 2^+ resonant state of the ^{14}Be nucleus. The three-body cluster model of ^{14}Be (^{12}Be + n + n) predicts that the valence neutrons will interact with the comparatively stable and inert ^{12}Be core. The three-body effective potential has a very large resonance width in the case of a shallow well with a wide thin barrier. When a particle's energy is close to resonance energy, it can be briefly trapped within the shallow well for a finite barrier height. But, there are fair chances that the particle to tunnel through the barrier. Hence, a precise resonance calculation of the huge width of resonance that results from a high chance of tunneling because of a low barrier height is easily used to conceal energy. Hence, we adopted the idea of the isospectral potential for the precise computation of resonance energy and resonance width.

Schrödinger equation involving three mutually interacting particles can be solved in relative coordinates using the HHE expansion approach [45] where the expansion of wave function in hyper-spherical harmonics (HH) and employment of orthogonality of HH yields a set of coupled differential equations (CDE) which is transformed into a single differential equation (SDE) in terms of an effective potential for the ground state energy, E_0, and wave function ψ_0 [46]. Following the prescription of the SSQM, we derive the isospectral potential. Finally, for various positive energies, we solve the SDE. The chance of discovering the particle trapped in the improved well-barrier is then calculated in terms of the trapping probability. The resonance energy corresponds to the prominent peak in the trapping-

probability versus energy plot. Back-transforming the wave function one can to compute the actual width of the resonance.

The paper is structured as follows. In section 2, we introduce the HHE approach briefly, we provided a brief overview of the SSQM process for creating the one-parameter family of isospectral potentials in section 3. In section 4, we discussed the results obtained in the current study. And finally, in section 5 we have drawn our conclusions.

2. Hyperspherical Harmonic Expansion (HHE) Method

The ^{14}Be is regarded as a (^{12}Be + n + n) system, with particle 1 being the core ^{12}Be and particles 2 and 3 being the two valence neutrons. Labeling scheme and Jacobi coordinate selection for a in general three-body configurations (CYY) in the partition "i", [i=1,2,3 - cyclic].

$$\vec{\alpha}_i = a_i\left(\vec{r}_j - \vec{r}_k\right); \vec{\beta}_i = \frac{1}{a_i}\left(\vec{r}_i - \frac{m_j\vec{r}_j + m_k\vec{r}_k}{m_j + m_k}\right) \tag{1}$$

Where $\vec{\chi} = \sum_{i=1}^{3} \frac{m_i r_i}{M}$ is the coordinate of the CM, M = (m_i + m_j + m_k) is the total mass of the system, and $\vec{\alpha}_i$ and $\vec{\beta}_i$ are defined by the constraint that i j, k form a cyclic permutation of (1, 2, 3). Khan (2012) [47] describes Jacobi coordinates are related to hyperspherical variables. in detail.

$$\alpha_i = \rho\cos\Phi_i;\ \beta_i = \rho\sin\Phi_i$$

Where $\rho = \sqrt{\alpha_i^{\,2} + \beta_i^{\,2}}; \Phi_i = \tan^{-1}\left(\frac{\beta_i}{\alpha_i}\right)$. The system's hyperspherical variables are the hyper radius ρ, this remains unchanged when particle indices are rotated and permuted in three dimensions, as well as the five angular variables Ω_i.

$$\left[\frac{-\hbar^2}{2\mu}\left\{\frac{\partial^2}{\rho^5} + \frac{5}{\rho}\frac{\partial}{\partial\rho} + \frac{\hat{K}^2\left(\Omega_i\right)}{\rho^2}\right\} + V\left(\rho, \Omega_i\right) - E\right]\Psi\left(\rho, \Omega_i\right) = 0 \tag{2}$$

Where $V\left(\rho, \Omega_i\right) = V_{jk} + V_{ki} + V_{ij}$ denotes the possibility for all interactions in partition i and $\hat{K}^2\left(\Omega_i\right)$ denotes the square of the hyper angular momentum operator that fulfils the eigenvalue equation

$$\widehat{K^2}\left(\Omega_i\right) Y K\left(\Omega_i\right) = K\left(K+4\right) Y_{K\delta_i}\left(\Omega_i\right) \tag{3}$$

The hyperangular momentum is denoted by the quantum number K and δ_i is a set of four quantum numbers associated with Jacobi coordinates. The hyperspherical harmonics (HH) are the partition dependent normalised eigenfunctions $Y\kappa_{\delta_i}\left(\Omega_i\right)$, which have a closed analytical expression. The wavefunction $\Psi\left(\rho, \Omega_i\right)$ is extended in the entire collection of hyperspherical harmonics connected to the partition " i " using the HHE approach.

$$\Psi\left(\rho, \Omega_i\right) = \sum_{\kappa_{\delta_i}} \frac{U\kappa_{\delta_i}\left(\rho\right)}{\rho^{5/2}} Y\kappa_{\delta_i}\left(\Omega_i\right) \tag{4}$$

The application of orthonormality of HH and the Eq. (4) being substituted in Eq (2) gives:

$$\left[\frac{-\hbar^2}{2\mu}\frac{d^2}{d\rho^2}+\frac{\left(\kappa+\frac{3}{2}\right)\left(\kappa+\frac{5}{2}\right)\hbar^2}{2\mu\rho^2}-E\right]U_{\kappa_{\delta_i}}(\rho)+\sum_{\kappa'\delta_i'}\kappa_{\delta_i}\left|V(\rho,\Omega_i)\right|\kappa'\delta_i'>U_{\kappa'\delta_i'}^{(\rho)}=0 \tag{5}$$

In principle, the set of CDEs, Eq. (5), is infinite because there are infinitely many basis states. Practically, the HH expansion in Eq. (4) is truncated by keeping all K values up to Kmax. The symmetry restrictions and related conserved quantum numbers also place a cap on the number of basis states. Hyperspherical adiabatic approximation (HAA) [48] is used to solve the reduced set of CDEs. HAA approximates the CDEs with a SDE, with the assumption that hyper radial motion(HRM) is substantially slower than hyper angular motion. As a result, the angular motion is solved first for a fixed ρ value. The system's energy is then determined by finding the hyper radial motion's effective potential by solving it for the lowest eigen potential $w_0(\rho)$.

$$\left[\frac{-\hbar^2}{2\mu}\frac{d^2}{d\rho^2}+w_0(\rho)-E\right]\Psi_0(\rho) \tag{6}$$

The algorithm for the renormalized Numerov technique is then used to solve Eq. (6) for $E\left(\leq E_0\right)$, with the proper boundary conditions i.e., $\rho\to 0$ and $\rho\to\infty$.

3. Isospectral Potential

The construction process for the one-parameter family of isospectral potential is briefly described in this section. In 1-D SSQM, the ground state wave function $\Psi_0(\rho)$ is used to define a super potential for the system [49]:

$$S(\rho)=\frac{-\hbar}{\sqrt{2\mu}}\frac{\Psi'_0(\rho)}{\Psi_0(\rho)} \tag{7}$$

The G.S. energy E_0 corresponding the potential $w_0(\rho)$ is then used to shift the energy scale, resulting in the new potential being

$$w_1(\rho)=w_0(\rho)-E_0=\frac{\hbar^2}{2\mu}\frac{\psi''}{\psi_0} \tag{8}$$

having a zero-energy ground state (i.e., $E_0^{(1)}=0$) The Ricatti equation can simply be used to check that $w_1(\rho)$ can be expressed using the superpotential.

$$w_1(\rho)=S^2(\rho)-\frac{\hbar}{\sqrt{2\mu}}S'(\rho) \tag{9}$$

Hamiltonian is now factorised as:

$$W_1=\frac{-\hbar^2}{2\mu}\frac{d^2}{d\rho^2}+w_1(\rho)=A^{'}A \tag{10}$$

$$\text{Where, } A^{'}=S(\rho)-\frac{\hbar}{\sqrt{2\mu}}\frac{d}{d\rho}\ \&\ A=S(\rho)+\frac{\hbar}{\sqrt{2\mu}}\frac{d}{d\rho} \tag{11}$$

which operators are used to create and destroy nodes in the wave function. Following that, we introduce a new partner Hamiltonian W_2, which corresponds to a new partner potential $w_2(\rho)$:

$$W_2=\frac{-\hbar^2}{2\mu}\frac{d^2}{d\rho^2}+w_2(\rho)=AA'; \tag{12}$$

$$w_2(\rho)=\mathrm{S}^2(\rho)+\frac{\hbar}{\sqrt{2\mu}}\mathrm{S}'(\rho) \tag{13}$$

Functions $w_1(\rho)$ and $w_2(\rho)$ in the preceding considered to be supersymmetric partner potentials.
Now we'll examine how W_1 and W_2's energy eigenvalues and wavefunctions are connected. It's worth noting that both W_1 and W_2 have positive semidefinite energy eigenvalues. The Schrodinger equation for W_1 for n > 0:

$$W_1\Psi_n^{(1)}=A^{'}A\Psi_n^{(1)}=E_n^{(1)}\Psi_n^{(1)}\ \&\ W_2\left(A\Psi_n^{(1)}\right)=AA^{'}A\Psi_n^{(1)}=E_n^{(1)}A\Psi_n^{(1)} \tag{14}$$

In the same way, the Schrodinger equation for W_2

$$W_2\Psi_n^{(2)}=AA'\Psi_n^{(2)}=E_n^{(2)}\Psi_n^{(2)}\ \&\ W_1\left(A'\Psi_n^{(2)}\right)=A'AA'\Psi_n^{(2)}=E_n^{(2)}A'\Psi_n^{(2)} \tag{15}$$

It is clear from Eqs. (14) and (15), as well as the fact that $E_0^{(1)}=0$ that the eigenvalues and eigenfunctions of the partner Hamiltonian W_1 and W_2 are connected by (n=0, 1, 2, 3, 4, 5,...

$$E_n^{(2)}=E_{n+1}^{(1)},E_0^{(1)}=0, \tag{16}$$

$$\Psi_n^{(2)}=\frac{1}{\sqrt{E_{n+1}^{(1)}}}\left(A\Psi_{n+1}^{(1)}\right), \tag{17}$$

$$\Psi_{n+1}^{(1)}=\frac{1}{\sqrt{E_{(n)}^{(2)}}}\left(A'\Psi_n^{(2)}\right) \tag{18}$$

The operator $A\left(A^{'}\right)$ establishes a new node in the eigenfunction as well as converting an eigenfunction of $W_1\left(W_2\right)$ into an eigenfunction of $W_2\left(W_1\right)$ utilising the same energy. Because the operator A annihilates W_1's ground state wave function, this state has no SUSY companion.
As can be seen from Eqs. (16) to (18), the Hamiltonians and have similar spectra, with the exception that the partner state of corresponding to the ground state of is missing from 's spectrum. As a matter of fact, the supersymmetric partner potentials and are not isospectral in the strictest sense. However, using the nonlinear nature of the Riccati equation (Eqs. (9) and (13)) and the superpotential are not unique, a family of strictly isospectral potentials with one parameter, called the λ can be created. There is a general superpotential that satisfies the Riccati equation.

$$\hat{S}(\rho)=S(\rho)+\frac{\hbar}{\sqrt{2\mu}}\frac{d}{d\rho}\ln\left[I_0(\rho)+\lambda\right] \tag{19}$$

Where λ is known as integration constant and

$$I_o(\rho)=\sum_{\rho'=0}^{\rho}\left[\psi_0(\rho')\right]^2d\rho' \tag{20}$$

$\psi_0(\rho)$ represents the normalised wave function of $w_0(\rho)$'s ground state. The potential

$$\widehat{w}_1(\lambda,\rho)=w_1(\rho)-\frac{\hbar^2}{2\mu}\left[\frac{4\psi_0(\rho)\psi_0(\rho)'}{I_0(\rho)+\lambda}-\frac{2\psi_0(\rho)^4}{\left(I_0(\rho)+\lambda\right)^2}\right] \tag{21}$$

then has the same SUSY Partner potential as well as the ground state with zero energy. Hence, $\widehat{w}_1(\lambda,\rho)$ is strictly isospectral to $w_1(\rho)$.

Numerically, an exact direct computation of the energy and width of any shallow potential function generated by the broad resonance is not possible. As a result, for E>0, using the $\psi(\rho)$ and Eqs. (20) and (21), the potential may be easily calculated:

$$\widehat{w}(\rho,\lambda)=w(\rho)-\frac{\hbar^2}{2\mu}\left[\frac{4\psi(\rho)\psi(\rho)}{I(\rho)+\lambda}-\frac{2\psi(\rho)^4}{\left(I(\rho+\lambda)\right)^2}\right] \tag{22}$$

We determine the chances of locating the system inside the potential well zone to precisely calculate the resonance energy,

$$P(E)=\int_{\rho'=0}^{\rho_B}\left[\widehat{\psi}_E(\rho',\lambda)^2\right]d\rho' \tag{23}$$

Utilizing energy time uncertainty relation, the resonance's width (Γ) is calculated from the state's mean lifetime. The decay constants inverse, or mean life, is equal. The formula for calculating Γ is as follows:

$$\Gamma=2\sqrt{\frac{\hbar^2}{2\mu}}\frac{\exp\left[-2\int_b^c\sqrt{\frac{2\mu}{\hbar^2}\left(\widehat{w}_1(\lambda,\rho)-E_R\right)}\right]}{\int_a^b\frac{dr}{\sqrt{\left[E_R-\widehat{w}_1(\lambda,\rho)\right]}}} \tag{24}$$

4. Application to ^{14}Be and the resulting data

Table 1. Energy (B= - E) calculated for the ^{14}Be ground state ($J=0^+$), together with the accompanying of relative convergence, the matter radius (R_m), and the partial impact of different l_x's on energy with rising K_{max}.

K_{max}	Energy (B= - E) (MeV)	Rel. Conv.	R_m (fm)	$-E_{l_\alpha}$(MeV)				
				$l_\alpha=0$	$l_\alpha=1$	$l_\alpha=2$	$l_\alpha=3$	$l_\alpha=4$
8	0.98268	0.16419	3.1293	0.67049	0.01570	0.19396	0.000120	0.03812
12	1.17572	0.03977	3.1247	0.82748	0.01587	0.22501	0.000127	0.04817
16	1.22442	0.01824	3.1216	0.87011	0.01681	0.23787	0.000131	0.05119
20	1.24716	0.00929	3.1196	0.89080	0.01886	0.24303	0.000133	0.05235
24	1.25886		3.1184	0.90086	0.01913	0.24518	0.000134	0.05273

$J=0^+$ describes the ^{14}Be ground state, while a resonance state of $J^\pi = 2^+$ exists. Hence, avoiding processes that begin with the ground state of ^{14}Be will result in $J^\pi = 2^+$ resonances. For the neutron-neutron pair, a typical GPT [50] potential is employed, whereas for the core neutron (^{12}Be - n) pair, a four-component SBB [51]. Gaussian type potential is used. The s-wave component of the SBB potential is retained repulsive to imitate the Pauli principle between core neutrons and additional core neutrons.

We used the hyperspherical extrapolation method (effectively implemented by Das et al., 1982 [46], Khan 2012 [47] to nuclear & atomic few-bodt calculations) to achieve a converged value of roughly 1.27 MeV for ^{14}Be at sufficiently large K_{max} because full energy convergence is not achieved at

K_{max}=24. Table 1 shows the calculated ground state energy and wavefunctions, as well as the RMS matter radii and relative convergence trend in ground energy of ^{14}Be with increasing basis size. Table 1 also computes the partial contributions of various partial waves to the ground state energy for l_α =0, 1, 2, 3, 4. The two-dimensional (2D) contour plot depicted in Fig. 1 shows that the low-density valence nucleons are widely spread, generating a halo-like shape, in contrast to the comparatively concentrated core nucleons that are more dense.

Table 2. The extrapolated energy ($B_{extrapolated}$) and also the corresponding tendency of relative convergence with the Kmax increase for bound ground state (J^π=0) of ^{14}Be.

K_{max}	$B_{extrapolated}$ (MeV)	Rel. Conv.	K_{max}	$B_{extrapolated}$ (MeV)	Rel. Conv.
24	1.2588619	0.004587307	76	1.2748264	0.000066436
28	1.2646633	0.002667567	80	1.2749111	0.000054589
32	1.2680459	0.001655711	84	1.2749807	0.000045332
36	1.2701489	0.001081537	88	1.2750385	0.000037879
40	1.2715241	0.000736211	92	1.2750868	0.000031968
44	1.2724609	0.000518333	96	1.2751276	0.000027134
48	1.2731208	0.000375471	100	1.2751622	0.000023134
52	1.2735990	0.000278581	104	1.2751917	0.000019918
56	1.2739539	0.000211109	108	1.2752171	0.000017173
60	1.2742229	0.000162896	112	1.2752390	0.000014977
64	1.2744305	0.000127570	116	1.2752581	0.000013095
68	1.2745931	0.000101434	----	-----	--------
72	1.2747224	0.000081579	∞	1.2754290	

Table 3. Parameters of the isospectral potential $\hat{w}(\lambda,\rho)$ as the λ decreases from $+\infty$ (For the original potential $w_0(\rho)$) in the direction of 0^+ of ^{14}Be.

λ	Potential Well		Potential Barrier	
	Depth (MeV)	Position (fm)	Height (MeV)	Position (fm)
∞	-1.8899	3.5990	1.4446	6.0179
100	-1.8919	3.5987	1.4597	6.0169
50	-1.8941	3.5962	1.4648	6.0160
1	-2.1019	3.5927	1.7318	5.9139
0.1	-3.8743	3.5530	1.8920	5.5049
0.01	-13.6448	3.2850	2.1366	5.3317
0.001	-40.2744	2.5620	12.0352	4.2299
0.0001	-91.2866	1.9850	36.5610	3.0730
0.00001	-161.2046	1.5520	81.1504	2.3530

Table 4. The following calculations for ^{14}Be were compared to data from experiments and other works of reference in the literature.

State	Observables	Present Work	Others Work	Reference
0^+			S_{2n} =1.26 ± 0.13 MeV	[52]
	Energy	E= -1.275 MeV	S_{2n} = 1.34 ± 0.11 MeV	[53]
	Matter radius	R_m = 3.1184 fm	R_m= 3.1 ± 0.4 fm,	[53]
			R_m= 3.10 ± 0.15 fm,	[54]
			R_m= 3.11 ± 0.38 fm	[55]
2_1^+	Resonance energy, E_R	E_R = 0.263 MeV	E_R = 0.28 MeV	[56]
			E_x = 1.54 ± 0.13 MeV	[56]
	Resonance width, Γ	Γ = 0.031 MeV	Γ = 0.025 MeV	[56]
2_2^+	Resonance energy, E_R	E_R = 2.273 MeV	E_R = 2.28 MeV	[56]
			E_x = 3.54 ± 0.16 MeV	[56]
	Resonance width, Γ	Γ = 1.489 MeV	Γ = 1.5 MeV	[56]

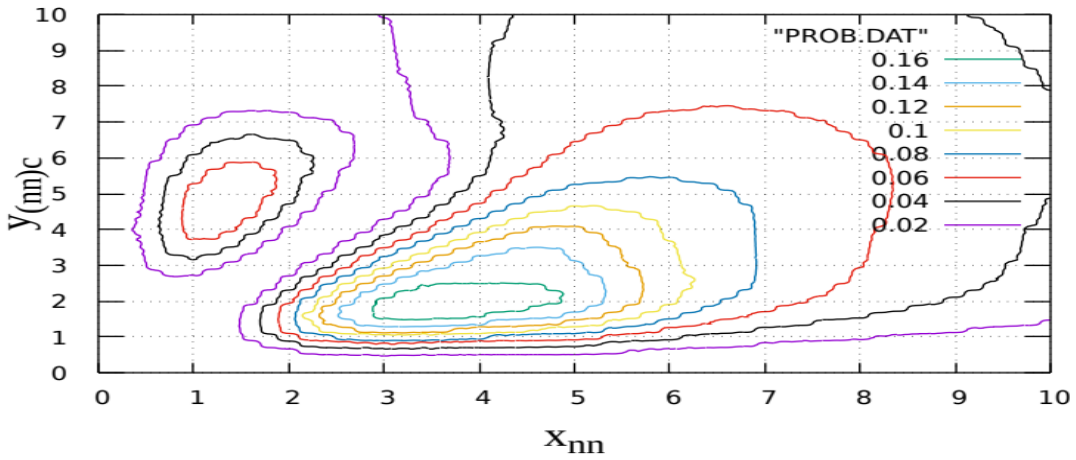

Figure 1. The density of correlation map for the g.s (0^+) of neutron dripline nucleus ^{14}Be in terms of Jacobi coordinates in two dimensions.

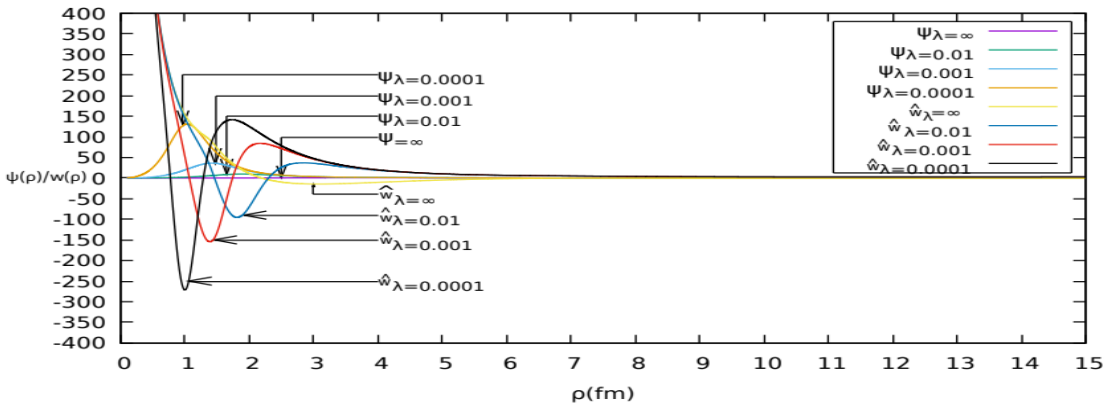

Figure 2. Isospectral potentials and wavefunctions for λ = ∞, 0.01, 0.001, and 0.0001 are graphically presented for ^{14}Be.

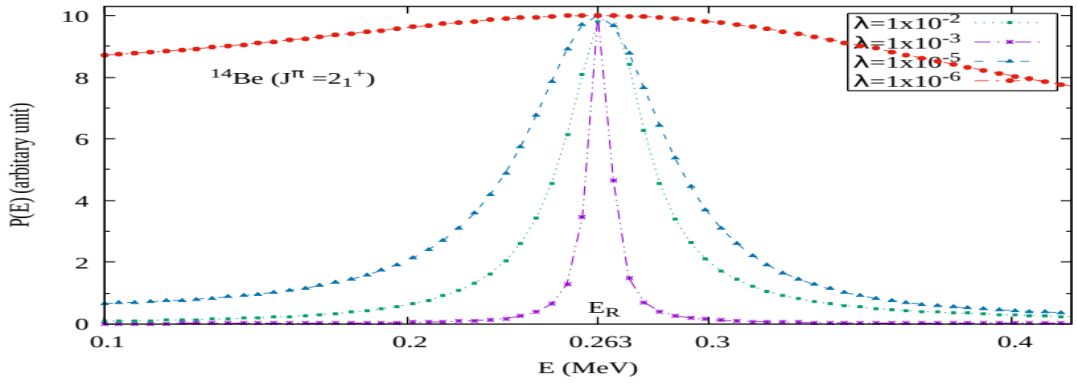

Figure 3. Graph illustrating the probability of trapping, P (E) Vs. E for the $J^{\pi}=2_1^+$ state of ^{14}Be to examine the resonance energy E_R.

As the value of λ approaches zero, the one-parameter of isospectral potential calculated using SSQM shows a dramatic effect. Table 3 shows the strengths and positions of the new constructed potential's minima and maxima. The potential well's depth rises from -3.87 MeV at 3.55 fm to -161.20 MeV at 1.55 fm when λ is reduced from 0.1 to 0.00001, while the height of the barrier increases from 1.89 MeV at 5.50 fm to 81.15 MeV at 2.35 fm. Figure 3 shows the estimated probability of particle trapping throughout the improved well-barrier combination shown in terms of E, exhibiting a resonance peak at E_R= 0.263 MeV for ^{14}Be. It's worth noting that the resonance energy is not affected by the free parameter λ. One of the key advantages of utilizing supersymmetric quantum mechanics algebra is that it improves the accuracy of determining resonance energy E_R.

5. Summary and Conclusions

Within this work, we have studied the bound and resonance states of the ^{14}Be nucleus in the context of a three-body (^{12}Be + n + n) cluster model adopting hyperspherical harmonics expansion formalism. The three-body Schrödinger equation in hyperspherical coordinates is numerically solved to obtain the wavefunction and ground state energy for the chosen set of GPT [50] n-n and SBB [51] core-n potential. The HHEM method used here is an essentially exact technique that involves no other approximation except an eventual truncation of the expansion basis due to the memory limitation of the available computer. However, we extrapolated the computed energy to get a fully

converged solution following the extrapolation technique used by Khan [47]. The contour plot of the probability density shown in Figure 1 clearly indicates a halo-like structure of ^{14}Be, in which the dense core (^{12}Be) is encircled by a low-density valence neutron envelope. As the original three-body effective potential has a shallow well following a low-wide barrier resulting in an excessively large resonance width, we invoked the principle of supersymmetric quantum mechanics (SSQM) to construct a one-parameter family of isospectral potential. For relatively smaller values of the free parameter (i.e., $\lambda \rightarrow 0+$), the isospectral potential develops a narrow and deep well following an enhanced barrier as shown in Figure 2. The system is effectively trapped by this improved well-barrier combination, giving rise to a sharp resonance that has the exact energy as the initial shallow potential. Thus the method is a robust one for the computation of resonances in weakly bound systems and even in unbound systems. The method can also be employed to search bound and resonances in exotic hypernuclei which may be formed near the nuclear landscape's neutron and proton drip lines. Conventionally, beyond the driplines, no bound nuclei can exist, but due to the capture of one or more strange hyperons by weakly bound or unbound nuclei, hypernuclei can be formed near the driplines. As there is no Pauli restriction between the captured hyperon(s) and the core nucleons, they can penetrate well inside the core nucleus forming a stable or quasi-stable hypernucleus. As summarized in Table 4, our computed ground state energy, RMS matter radii, resonance energy, and resonance width data are all in good agreement with those found in the literature, thereby accomplishing our goal set for this work.

Acknowledgments

The authors are thankful to Aliah University, Kolkata, India, for providing the computational facilities. One of the Authors is wishing to acknowledge the University Grants Commission, Government of India, New Delhi for providing financial assistance.

References

[1] Kobayashi N et al. 2012 Physical Review C. **86** 054604
[2] Hwash W S 2017 Turk. Jour. Phys. **41** 151-159
[3] Schwab W et al. 1995 Z. Physik A – Had. and Nucl. **350** 283-284
[4] Tanihata I et al. 1985 Physical Review Lett. **55** 2676
[5] Khalili J S Al and Tostevin J A 1996 Physical Review Lett. **76** 3903
[6] Fukuda M et al. 2014 EPJ Web Conferences, **66** 02037
[7] Abdullah A N 2020 Int. Jour. Mod. Phys. E, **29** 2050015
[8] Khan M A et al. 2021 Few-Body Syst. **62** 54
[9] Jensen A S and Riisager 2000 Physics Letter B, **480** 39-44
[10] Tanaka K et al. 2010 Physical Review Lett. **104**, 062701
[11] Acharya B and Phillips D R 2013 Nuclear Physics A, **913** 103-115
[12] Descouvemont P 1999 Nuclear Physics A **655** 440
[13] Hamamoto I 2010 Physical Review C **81** 021304 (R)
[14] Liu Q, Guo J Y, Niu Z M and Chen S W 2012 Physical Review C **86** 054312
[15] Tian Y J, Liu Q, Heng T H and Guo J Y 2017 Physical Review. C **95** 064329
[16] Takechi M *et al. 2014* Physical Review C **90**, 061305(R)
[17] Hamamoto I 2017 Physical Review C **95**, 044325

[18] Bang J M et al. 1996 Physics Report **264** 27
[19] Banerjee P et al. 1998 Physical Review C **58** 1337
[20] Brodeur M et al. Physical Review Lett. **108** 052504
[21] Sun Y L 2021 Physics Letter B **814** 136072
[22] Souza L A et al. 2016 Physics Letter B **757** 368
[23] Hwash W S et al. 2012 Intr. Jour. Mod. Phys. E **21** 1250066
[24] Canham D L et al. 2008 Euro Physics Jour. A **37** 367
[25] Labiche et al. 2001 Physical Review Lett. **86** 600
[26] Ren Z et al. 1995 Physics Letter B **351** 11
[27] Hasan M et al. 2019 Jour. Phys. Conf. Ser. **1354** 012003
[28] Togano Y et al. 2016 Physics Letter B **761** 412
[29] Gaudefroy L et al. 2012 Physical Review Lett. **109** 202503
[30] Khan M A et al. 2021 Nuclear Physics A **1015** 122316
[31] Zhang K Y et al. 2019 Physical Review C **100** 034312
[32] Fukuda M et al. 1999 Nuclear Physics A **656** 209
[33] Ren Z et al. 1996 Physical Review C **53** R572(R)
[34] Ibraheem A A et al. 2019 Rev. Mex. Fiz. **65** 168
[35] Cai X Z et al. 2002 Physical Review C **65** 024610
[36] Tanaka K et al. 2005 Euro Physics Jour. A **25** 221
[37] Gilman R et al. 1984 Physical Review C **30** 958
[38] Wouters J M et al. 1988 Z. Phys. A **331** 229
[39] Audi G and Wapstra, 1993 Nuclear Physics A **565** 193
[40] Moriguchi T et al. 2014 Nuclear Physics A **929** 83-93
[41] Sugimoto T et al. 2007 Physics Letter B **654** 160-164
[42] Korsheninnikov A A et al. 1997 Nuclear Physics A **616** 189-200
[43] Bohlen H G et al. 1995 Nuclear Physics A **583** 775
[44] Kisamori K et al. 2016 Physical Review Lett. **116** 052501
[45] Ballot J L et al. 1982 Annu. Phys. **127** 62
[46] Das T K et al. 1982 Physical Review C **26** 2281
[47] Khan M A, 2012 Euro Phys. Jour. D **66** 83
[48] Khan M A and Das T K, 2001 Pramana Jour. Phys. **57** 701
[49] Cooper F et al. 1995 Physics Report **251** 267
[50] Gogny D, Pires P and Tourreil R D, 1970 Physics Letter **32B** 591
[51] Sack S, Biedenham L C and Breit G, 1954 Physical Review **93** 321
[52] Audi G et al. 2003 Nuclear Physics A **729** 337
[53] Zahar M et al. 1993 Physical Review C **48** R1484
[54] Suzuki T et al. 1999 Nuclear Physics A **658** 313
[55] Tanihata I et al. 1988 Physics Letter B **206** 592
[56] Aksytina Y et al. 2013 Physical Review Lett. **111** 242501